Mechanistic Investigation of the Heterogeneous Hydrogenation of Nitrite over Pt/Al2O3 by Attenuated Total Reflection Infrared Spectroscopy

ARTICLE *in* THE JOURNAL OF PHYSICAL CHEMISTRY C · JANUARY 2009

Impact Factor: 4.77 · DOI: 10.1021/jp8081886

3 AUTHORS:

Sune Dalgaard Ebbesen
Innovation Fund Denmark
65 PUBLICATIONS **1,426** CITATIONS
SEE PROFILE

Barbara L Mojet
University of Twente
80 PUBLICATIONS **1,801** CITATIONS
SEE PROFILE

Leon Lefferts
University of Twente
196 PUBLICATIONS **3,597** CITATIONS
SEE PROFILE

Mechanistic Investigation of the Heterogeneous Hydrogenation of Nitrite over Pt/Al_2O_3 by Attenuated Total Reflection Infrared Spectroscopy

Sune D. Ebbesen,[†] Barbara L. Mojet, and Leon Lefferts*

Catalytic Processes and Materials, Faculty of Science and Technology, Institute of Mechanics Processes and Control Twente (IMPACT) and MESA$^+$ Institute for Nanotechnology, University of Twente, P.O. Box 217, 7500 AE, Enschede, The Netherlands

Received: September 15, 2008; Revised Manuscript Received: November 27, 2008

The mechanism of the heterogeneous hydrogenation of nitrite over a Pt/Al_2O_3 catalyst layer deposited on a ZnSe internal reflection element was investigated in water using attenuated total reflection infrared spectroscopy. In addition to adsorbed nitrite, hydrogenation intermediates $NO_{(ads)}$, "HNO"$_{(ads)}$, and $HNO_2^-{}_{(ads)}$ are formed on the platinum surface. Hydrogenation of the surface intermediates mainly results in NH_4^+, but also traces of N_2O are observed as well, which is believed to be an intermediate in the formation of nitrogen. "HNO"$_{(ads)}$ is the most prominent surface species during steady state operation and is therefore involved in the rate-determining step. Some $NO_{(ads)}$ accumulates at steps in transient experiments, showing a very low reactivity toward N_2O. The results show that although the reaction pathways of nitrite hydrogenation on platinum and palladium are rather similar; the rate-determining steps on the metals are clearly different.

Introduction

Groundwater pollution by nitrate and nitrite is a widespread problem and is worldwide a potential risk to human health. High concentrations of nitrate and nitrite in drinking water can be fatal for infants, as nitrate and nitrite can cause the blue baby syndrome.[1] Furthermore, nitrate can be converted into nitrosamine, which can cause cancer and hypertension.[1] In recent years, nitrate and nitrite concentrations in groundwater increased at many locations throughout the world, and consequently wells have to be shut down.[2,3] As a result, there is a renewed interest in processes for removal of nitrite and nitrate from groundwater.

Most promising is the heterogeneous hydrogenation over palladium and platinum catalysts, which have been studied extensively.[4−11] In general, it is accepted that the same reaction mechanism holds for both palladium and platinum catalysts; nitrite is hydrogenated to nitrogen and ammonia with adsorbed NO as an intermediate.[5,6,12−16] Palladium catalysts show higher selectivity to nitrogen than platinum catalysts.[4,7,17] Attenuated total reflection infrared spectroscopy (ATR-IR) is ideally suited for studying molecular vibrations at the solid−liquid interface because the evanescent wave is restricted to the region near the interface, thereby minimizing the contribution from the liquid.[18] Recently, ATR-IR spectroscopic studies at the metal−liquid interface have started to receive attention.[15,19−26] We have recently applied ATR-IR spectroscopy to study the adsorption behavior of nitrite, hydroxylamine (NH_2OH) and ammonia on both Pd/Al_2O_3 and Pt/Al_2O_3.[23] In addition, we have studied the reaction mechanism of nitrite hydrogenation over Pd/Al_2O_3.[15] Nitrite and ammonia adsorb both on passivated Pt/Al_2O_3 and Pd/Al_2O_3, while hydroxylamine decomposes on the catalysts. On Pt/Al_2O_3, NH_2OH decomposes to a species, which is most likely adsorbed HNO that decomposes to adsorbed NO. On Pd/Al_2O_3, on the other hand, NH_2OH decomposes to form a stable $NH_{2(ads)}$ fragment. This $NH_{2(ads)}$ adsorbate was also observed during continuous hydrogenation of nitrite over Pd/Al_2O_3, along with NO and NH_4^+ on the palladium surface.[15] Formation of ammonia was found to proceed solely via hydrogenation of adsorbed NH_2, whereas the hydrogenation product of adsorbed NO could not be detected. N_2, which is not infrared active, was regarded as the most likely hydrogenation product of $NO_{(ads)}$.[15] On the basis of these findings a reaction mechanism involving two parallel hydrogenation reactions on palladium (i.e., hydrogenation of NO to N_2 and hydrogenation of NH_2 to NH_4^+) was suggested.[15]

In contrast to the parallel hydrogenation reactions suggested for Pd/Al_2O_3, a single stepwise hydrogenation process of nitrite was proposed for the electrochemical reduction of nitrite over platinum electrodes.[27] Several papers report on the experimental evidence of adsorbed NO as an intermediate during electrochemical reduction of nitrate and nitrite over platinum.[28−33] The subsequent electrochemical reduction of adsorbed NO mainly yielded ammonia, although traces of N_2O have also been detected. In addition, N_2O was demonstrated to be an intermediate in the formation of nitrogen.[34,35]

Clearly, electrochemical studies cannot be compared directly to catalytic studies. Electrochemical studies are confined to dense conducting electrodes, often single crystals, instead of practical catalysts containing supported metal nanoparticles on porous support materials. It is well-known that the difference in the structure of the metal surface can induce significant differences in the chemical and catalytic properties.

It is the objective of this study to examine the surface intermediates during hydrogenation of nitrite over Pt/Al_2O_3 by in situ ATR-IR spectroscopy, to obtain insight in the mechanism of the heterogeneous hydrogenation of nitrite over Pt/Al_2O_3. Also, similarities and differences between hydrogenation of nitrite over Pt/Al_2O_3 and Pd/Al_2O_3 will be discussed.

Experimental Section

Catalyst Preparation and Characterization. First, a 5 wt % Pt/Al_2O_3 powder catalyst was prepared and characterized.

* To whom correspondence should be addressed. E-mail: L.Lefferts@utwente.nl. Phone: + 31 53 489 2858. Fax: +31 53 489 4683.

† Present address: Fuel Cells and Solid State Chemistry Department, Risø - DTU National Laboratory for Sustainable Energy, Frederiksborgvej 399, DK-4000 Roskilde, Denmark.

10.1021/jp8081886 CCC: $40.75
Published on Web 01/20/2009

Next, the catalyst powders was deposited on a ATR-IR ZnSe internal reflection element (IRE) and mounted in an in situ ATR-IR cell as previously described.[15,20,23,36,37] In short, precalcined γ-Al_2O_3 powder was impregnated with a solution of $H_2PtCl_6 \cdot 6H_2O$ (Alfa Aesar) to yield a catalyst with 5 wt % platinum loading (details can be found in a previous papers[20,37]) The slurry was mixed for 2 h and was followed by drying at 335 K for 2 h in a rotating evaporator. The impregnated Pt/Al_2O_3 powder was then calcined at 673 K for 3 h (heating rate 5 K/min) in synthetic air (30 mL/min) and reduced at 673 K for 3 h (heating rate 5 K/min) in hydrogen (30 mL/min). The platinum dispersion for the 5 wt % Pt/Al_2O_3 catalyst was determined at 75% by hydrogen chemisorption.

A suspension of Pt/Al_2O_3 was prepared from 0.3 g of Pt/Al_2O_3 in 50 mL of water; pH was adjusted to 3.5 with nitric acid to stabilize small alumina particles. The suspension was milled for 1 h in a ball-mill (Fritsch Pulverisette) to obtain particles of a few nanometers in size. Subsequently, colloidal alumina corresponding to 5 wt % of the catalyst amount was added (aluminum oxide, 20% in H_2O colloidal suspension, Alfa Aesar, particle size 5 nm). The catalyst layer was prepared on the IRE by adding 1 mL of the catalyst/water suspension evenly on one side of the IRE. The suspension was allowed to evaporate overnight at room temperature. Subsequently, the catalyst layer/IRE was heated to 573 K for 2 h (heating rate 1 K/min) in flowing argon followed by reduction at 673 K (in hydrogen, heating/cooling rate 10 K/min) to ensure removal of all NO_x species on the catalyst surface. About 6 mg of catalyst was deposited on the IRE. The thickness of the Pt/Al_2O_3 catalyst layer was 3.5 ± 0.25 μm.[20] The prepared Pt/Al_2O_3 catalyst layer contained in total 1.2×10^{-6} mol accessible surface platinum atoms within the cell, based on the platinum dispersion of 75%.

In Situ ATR-IR Spectroscopy. The water used in all ATR-IR experiments was ultrapure Q2-water, prepared with a Millipore Milli-Q water treatment system from Amphotech Ltd. Saturation of water with Ar (5.0, Praxair), or H_2 (5.0, Praxair), was performed at room temperature (294 K) with gas flow rates of 40 mL min^{-1} for a minimum of two hours. Prior to saturation with H_2, air was removed by saturation with argon for at least two days. The concentrations of dissolved gases in water were calculated based on reported solubility data at room temperature and 1 atm gas pressure.[26] The Q2-water saturated with Ar (2.3×10^{-3} mol$\cdot$$L^{-1}$) or H_2 (4.1×10^{-4} mol$\cdot$$L^{-1}$) are designated as, respectively, Ar/H_2O or H_2/H_2O in the following. A solution of $NO_2^-{}_{(aq)}$ (4.3×10^{-4} mol$\cdot$$L^{-1}$) was prepared in Ar/$H_2O$ from $NaNO_2$ (Merck). pH was adjusted to 7.0 by adding NaOH (Merck); pH was measured using a pH meter (744 pH meter, Metrohm). For the continuous hydrogenation experiments, the nitrite solution was subsequently saturated with a mixture of hydrogen and argon to obtain the respective hydrogen concentrations.

ATR-IR spectra were recorded using a home-built stainless steel flow-through cell as described elsewhere.[17,23−25] The flow-through chamber was created by a spacer placed between the polished steel top-plate and the IRE. The thickness of the spacer was 0.3 mm; the length and width of the exposed area of the coated IRE were 40 × 10 mm, respectively. The total volume of the cell was 120 μL. The liquid flow rate was 1 mL$\cdot$$min^{-1}$ in all experiments; as a result, the residence time in the cell was 7.2 s. Further, taking the accessible Pt surface atoms into account (1.2×10^{-6} mol, vide ante) it will take approximately 3 min to add stoichiometric amounts of H_2 and/or NO_2^- to the cell (at a hydrogen/nitrite concentration of $4.1-4.3 \times 10^{-4}$ mol/L, see above).

The ATR-IR cell was assembled with the coated IRE and mounted in the sample compartment of an infrared spectrometer (Bruker Tensor 27) equipped with a MCT detector. After assembling the cell in the IR spectrometer, the cell was flushed with Ar/H_2O until a stable water spectrum was obtained. Subsequently, the catalyst was reduced in situ by introducing H_2/H_2O (4.1×10^{-4} mol/L H_2); this catalyst is denoted H−Pt/Al_2O_3. Also some experiments were performed on a fresh Pt/Al_2O_3 catalyst layer, which was not reduced in the ATR cell. This catalysts is denoted Pt/Al_2O_3.

All ATR-IR spectra were recorded at room temperature (294 K) in an air-conditioned room. IR spectra were recorded by averaging of 128 scans with a resolution of 4 cm^{-1}, which took about 78 s. This is approximately 10 times longer than the liquid residence time in the cell. Thus, each spectrum represents the overall changes in the spectra over a period of about 78 s. The interval between the start of two subsequent spectra was 90 s. As a result, the time resolution between the spectra was 90 s.

Data Treatment. As shown by our group, the ATR-IR spectra must be corrected for the infrared absorbance of water.[36] The subtraction used in the present study is performed by subtracting a scaled background for dissolved gases as previously described.[20,36,37] To calculate the respective peak areas, curve fitting was applied after subtraction of the water spectra. The curve fitting was performed based on a Lorentzian function. The applied Lorentzian line-shape function centered at the frequency $\omega_0$is given by

$$I(\omega) = A\,\frac{2}{\pi}\,\frac{w}{4(\omega-\omega_0)+w^2}$$

where $I(\omega)$ is the intensity at a given frequency ω, A the integrated area, and w the full width at half of the maximum intensity.

Results and Discussion

In the following sections a variety of experiments will be described and discussed which all together lead to a better insight in the mechanism of nitrite reduction over Pt/Al_2O_3. In a previous paper we have shown that adsorption of $NO_2^-{}_{(aq)}$ (at 1235 cm^{-1}) on passivated platinum leads to two different adsorbed NO_x species on the platinum surface, observed at respectively 1390 and 1305 cm^{-1}.[23,27] These peaks will be denoted as $NO_x^{-1305\ cm^{-1}}{}_{(ads)}$ and $NO_x^{-1390\ cm^{-1}}{}_{(ads)}$ in the following.

In this paper we show the adsorption and reaction of $NO_2^-{}_{(aq)}$ on H−Pt/Al_2O_3, followed by reduction of the produced surface species. Further, the reduction of adsorbed $NO_x^{-1305\ cm^{-1}}{}_{(ads)}$ and $NO_x^{-1390\ cm^{-1}}{}_{(ads)}$ will be discussed, which clearly shows that different reaction pathways exists, depending on the surface species present at the start of the hydrogenation. At the end, the continuous hydrogenation of nitrite over Pt/Al_2O_3 will be presented. All the results end up in a reaction network, which will be discussed in comparison with the mechanism over Pd/Al_2O_3 published recently.[15]

Adsorption of $NO_2^-{}_{(aq)}$ on H−Pt/Al_2O_3. First, the surface reaction between nitrite and preadsorbed hydrogen was studied by exposing H−Pt/Al_2O_3 to $NO_2^-{}_{(aq)}$ (4.3×10^{-4} mol/L) at pH 7. Infrared peaks evolved as shown in part A; the integrated peak areas obtained by curve fitting are shown in parts B and C of Figure 1.

Initially peaks developed at 2231, 1540, 1455, 1390, and 1305 cm^{-1}. Further a shoulder was observed at 1235 cm^{-1}. During continuous flow of $NO_2^-{}_{(aq)}$, the band at 1455 cm^{-1} disappeared in approximately 10 min. At the same time, gradually a new peak appeared at 1570 cm^{-1}, which shifted to 1580 cm^{-1} with

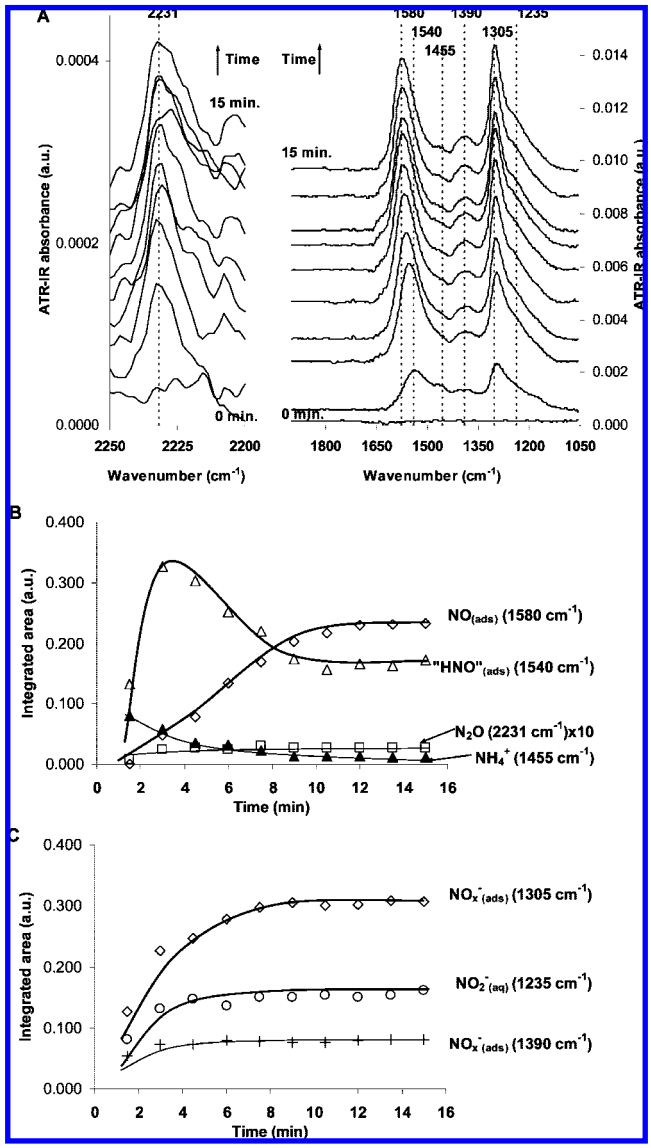

Figure 1. (A) Water-corrected ATR-IR spectra while flowing a solution of $NO_2^-{}_{(aq)}$ (4.3×10^{-4} mol/L) over H−Pt/Al_2O_3 at pH 7.0. (B and C) Integrated peak areas of observed species during $NO_2^-{}_{(aq)}$ flow.

increasing intensity. Simultaneously, the peak at 1540 cm^{-1} reached a maximum after 3 min, subsequently decreased, and stabilized after 10 min. [Note: in ref 23, we have shown that the two peaks at 1580 cm^{-1} and 1540 cm^{-1} belong to different species since they can be converted into each other in the presence/absence of hydrogen.]

On the basis of the results of our previous paper, these peaks can be assigned as follows. The peak at 2231 cm^{-1} is assigned to N_2O,[23,29,34,37−40] which is dissolved or weakly adsorbed at the catalyst surface. It should be noted that despite its very low intensity (50 times lower than ammonia at 1455 cm^{-1}), the band of N_2O still can be observed.

The band at 1570 cm^{-1}, shifting to 1580 cm^{-1}, originates from bridged adsorbed NO at low coverage on the platinum surface,[23,28,29,37] denoted as $NO_{(ads)}^{1580\ cm^{-1}}$ in the following. At 1540 cm^{-1}, "HNO"$_{(ads)}$ is found, and the band at 1455 cm^{-1} is assigned to NH_4^+.[23,27] No distinction can be made between dissolved NH_4^+ and NH_4^+ adsorbed on the catalyst surface based on the IR spectrum. As said above, the peaks at 1390 and 1305 cm^{-1} arise from adsorbed NO_x species on the platinum surface, and the peak at 1235 cm^{-1} is due to NO_2^- in the solution.[23,37]

Figure 1 shows that the intensity of $NO_2^-{}_{(aq)}$ (1235 cm^{-1}) and $NO_x^-{}_{(ads)}^{1305\ cm^{-1}}$ stabilized after several minutes, which is much longer than the residence time in the cell of 7.2 s. The effect is most significant for $NO_x^-{}_{(ads)}^{1305\ cm^{-1}}$, for which it takes almost 10 min to stabilize. This is due to the adsorption and conversion of nitrite by adsorbed hydrogen on the platinum surface, resulting in the hydrogenation products NH_4^+, "HNO"$_{(ads)}$, N_2O, and $NO_{(ads)}^{1580\ cm^{-1}}$, and adsorbed NO_x^- species. Since $NO_x^-{}_{(ads)}^{1305\ cm^{-1}}$ reaches its maximum intensity after the signals for "HNO"$_{(ads)}$, $NO_{(ads)}^{1580\ cm^{-1}}$, and NH_4^+ leveled off, we propose the following reaction sequence

$$NO_{x(ads)}^{-1305cm^{-1}} \xrightarrow{H_2} NO_{(ads)}^{1580cm^{-1}} \overset{H_2}{\rightleftharpoons} \text{"HNO"}_{(ads)} \xrightarrow{H_2} NH_{4(ads)}^+ \qquad (1)$$

At the start of the experiment, the surface coverage of hydrogen is high and "HNO"$_{(ads)}$ and NH_4^+ are mainly produced, whereas $NO_{(ads)}^{1580\ cm^{-1}}$ starts to develop after 3 min. It was shown before that "HNO"$_{(ads)}$ and $NO_{(ads)}^{1580\ cm^{-1}}$ are in equilibrium, depending on the H_2 concentration.[23]

The formation of ammonia during the catalytic hydrogenation of nitrite is well documented, and platinum catalysts are known to be selective toward ammonia for this reaction.[4,7,17] The high initial formation of ammonia, when adsorbing $NO_2^-{}_{(aq)}$ on H−Pt/Al_2O_3 with high hydrogen coverage, is further in agreement with the observation that selectivity to ammonia increases with higher hydrogen concentration.[4,5,11,41,42] After approximately 10 min the formation rate of NH_4^+ is close to zero and the concentrations of $NO_{(ads)}^{1580\ cm^{-1}}$ and "HNO"$_{(ads)}$ stabilize, presumably because there is no hydrogen available anymore for further hydrogenation. After 15 min of $NO_2^-{}_{(aq)}$ flow over H−Pt/Al_2O_3 (Figure 1), the cell was flushed with Ar/H_2O for 5 min to remove $NO_2^-{}_{(aq)}$. When flowing Ar/H_2O, $NO_2^-{}_{(aq)}$ (1235 cm^{-1}) was completely flushed out of the cell within 90 s (not shown). In addition, a slight increase in the peak for $NO_{(ads)}^{1580\ cm^{-1}}$was observed (+7%), along with a minor decrease in the peaks for "HNO"$_{(ads)}$ (−5%) and $NO_{x\ (ads)}^{-1305\ cm^{-1}}$ (−10%). These changes are in agreement with our previous study, in which we showed that "HNO"$_{(ads)}$ decomposes into $NO_{(ads)}^{1580\ cm^{-1}}$ during inert flow.[23,37] Remarkably, even after inert water flow, N_2O is still being detected at a very low intensity. Since we recently showed that dissolved N_2O in the water in the pores and voids in the catalysts layer is immediately removed when Ar/H_2O is introduced, the results here indicate that N_2O is continuously produced. Most likely, N_2O is formed from either dimerization of $NO_{(ads)}^{1580\ cm^{-1}}$ or "HNO"$_{(ads)}$ or a reaction between $NO_{(ads)}$ and adsorbed "HNO"$_{(ads)}$, as we have previously discussed.[23,37] However, the fact that the amounts of $NO_{(ads)}^{1580\ cm^{-1}}$ and "HNO"$_{(ads)}$ hardly change, and the very low intensity of the N_2O band indicate that the reaction rate must be very low.

Hydrogenation of $NO_{(ads)}^{1580\ cm^{-1}}$, "HNO"$_{(ads)}$, and $NO_x^-{}_{(ads)}$ on H−Pt/Al_2O_3. After adsorption of $NO_2^-{}_{(aq)}$ on H−Pt/Al_2O_3 and flushing with Ar/H_2O, $NO_{(ads)}^{1580\ cm^{-1}}$, "HNO"$_{(ads)}$, and $NO_x^-{}_{(ads)}$ remained adsorbed on the platinum surface which were subsequently exposed to H_2/H_2O to study their reactivity to hydrogen. Figure 2 shows the infrared spectra with time and the associated integrated peak areas.

First, the peak for $NO_{(ads)}^{1580\ cm^{-1}}$started to decrease, while simultaneously the peak for "HNO"$_{(ads)}$ (1540 cm^{-1}) increased. The peak intensity for NH_4^+ (1455 cm^{-1}) remained very low until around 4 min, where after it slowly increased until 10 min when the band of "HNO"$_{(ads)}$ reached a maximum, and

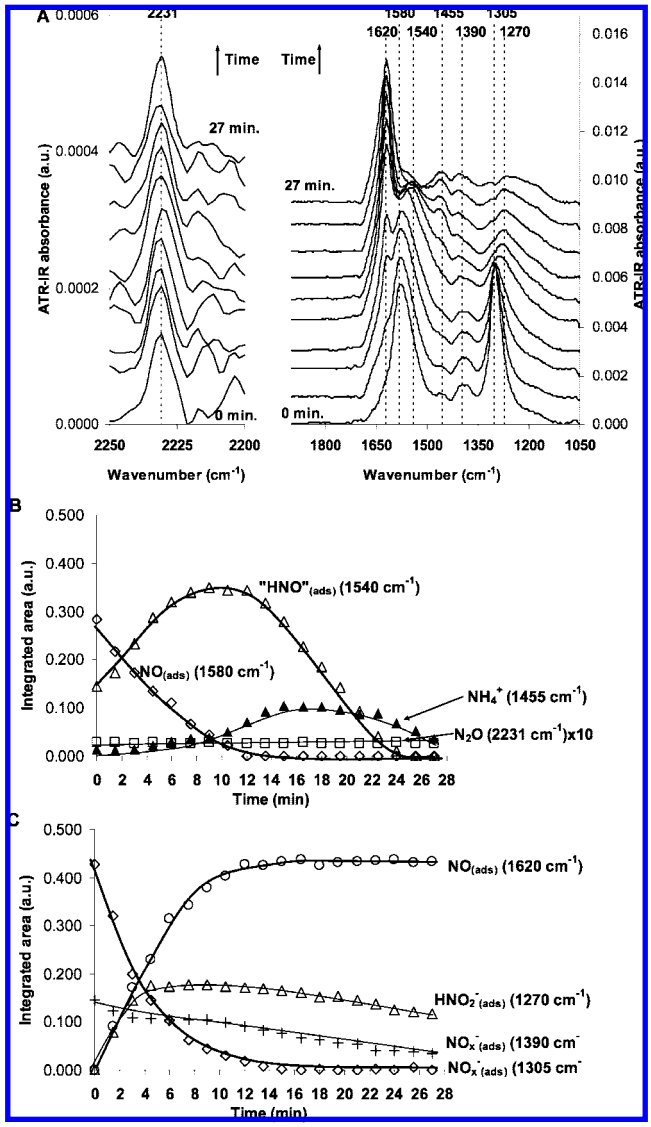

Figure 2. (A) Water-corrected ATR-IR spectra while H_2/H_2O (4.1×10^{-6} mol/L H_2) was flown over Pt/Al_2O_3 with of N_2O, "HNO"$_{(ads)}$, and $NO_x^-{}_{(ads)}$, previously formed during adsorption of $NO_2^-{}_{(aq)}$ on H−Pt/Al_2O_3 (Figure 1). (B and C) Integrated peak areas during flow of H_2/H_2O.

$NO_{(ads)}^{1580\ cm^{-1}}$ completely had disappeared. Subsequently, the peak for "HNO"$_{(ads)}$ decreased with a simultaneous quicker increase of the NH_4^+ peak up to 18 min, after which it started to decrease slowly.

In Figure 2, it can clearly be seen that the two adsorbed nitrite species, $NO_x^{-1390\ cm^{-1}}{}_{(ads)}$ and $NO_x^{-1305\ cm^{-1}}{}_{(ads)}$ respond differently to the exposure of hydrogen. The $NO_x^{-1390\ cm^{-1}}{}_{(ads)}$ band decreases much slower than the peak for $NO_x^{-1305\ cm^{-1}}{}_{(ads)}$, demonstrating that these two peaks arise from two different adsorbed NO_x^- species, as we previously discussed as well.[23,37]

In addition to the bands already assigned, two new peaks appeared during the reduction of $NO_{(ads)}^{1580\ cm^{-1}}$, "HNO"$_{(ads)}$, and $NO_x^-{}_{(ads)}$ on Pt/Al_2O_3. First, an asymmetric peak developed at 1270 cm^{-1}, which decreased slowly with time after a few minutes. The band at 1270 cm^{-1} was reported in electrochemical studies on nitrate hydrogenation on platinum electrodes and was assigned to $HNO_2^-{}_{(ads)}$.[29] Since hydrogenation of NO_2^- to $HNO_2^-{}_{(ads)}$ is a reasonable proposition and no other assignments could be found in literature, the peak at 1270 cm^{-1} is assigned to $HNO_2^-{}_{(ads)}$ on the platinum surface. The intensity of this species is moderately low, and it can only be detected via curve fitting in the presence of $NO_x^{-1305\ cm^{-1}}{}_{(ads)}$ and $NO_2^-{}_{(aq)}$ which have relatively intense bands at similar wave numbers.

Second, a new peak appeared at 1620 cm^{-1} which reached a constant maximum after 12 min. This peak is distinctively different from $NO_{(ads)}^{1580\ cm^{-1}}$, which was identified as bridged NO.[23,28,29,37] Its frequency is too low to originate from linearly adsorbed NO on Pt(111), which is reported at 1680 cm^{-1}.[23,30,33,37] In literature, the band at 1620 cm^{-1} has been assigned to $NO_{(ads)}$ on a Pt(100) surface characterized by steps.[30] In our study, however, the heterogeneous supported platinum particles exhibit a variety of crystal planes, steps, and edges, which limits the exact assignment of the peak to a specific crystal surface. Further, the band at 1620 cm^{-1} does not show a shift with increasing intensity (Figure 2), pointing to the absence of dipole−dipole coupling. Moreover, the 1620-cm^{-1} species is extremely stable, in other words it does not dissociate on the time scale investigated. These two phenomena lead to the conclusion that NO is adsorbed on isolated step sites. As a result, the band at 1620 cm^{-1} is assigned to NO adsorbed on steps, denoted as $NO_{(steps)}^{1620\ cm^{-1}}$.

The concentration of $NO_{(steps)}^{1620\ cm^{-1}}$ very slowly decreased (less than 10% in 24 h) during continued H_2/H_2O exposure (not shown), indicating a low reactivity toward hydrogen. This is in agreement with literature reporting the electrochemical reduction of both nitrite and NO adlayers being structure sensitive,[43−45] and NO was suggested to accumulate at steps during electrochemical reduction of nitrate over platinum electrodes.[43]

At this point, it is not clear from which species the $NO_{(steps)}^{1620\ cm^{-1}}$ adsorbate is formed. During decomposition of hydroxylamine on Pt/Al_2O_3, both "HNO"$_{(ads)}$ and $NO_{(ads)}^{1580\ cm^{-1}}$ were found, while no $NO_{(steps)}^{1620\ cm^{-1}}$ was observed.[23,37] That result suggests that the production of $NO_{(steps)}^{1620\ cm^{-1}}$ possibly occurs via direct hydrogenation of NO_x^- and/or via $HNO_2^-{}_{(ads)}$ as clearly observed in the present study. To investigate the origin and role of $NO_{(steps)}^{1620\ cm^{-1}}$ in the hydrogenation of nitrite over Pt/Al_2O_3, additional experiments were carried out starting from a passivated Pt/Al_2O_3 (without preadsorbed hydrogen).

Hydrogenation of Preadsorbed NO_2^- on Pt/Al_2O_3. In the experiment described above, already four adsorbates were present on the platinum surface, $NO_{(ads)}^{1580\ cm^{-1}}$, "HNO"$_{(ads)}$, $NO_x^{-1390\ cm^{-1}}{}_{(ads)}$, and $NO_x^{-1305\ cm^{-1}}{}_{(ads)}$, which were exposed to hydrogen at the same time. To understand the reactivity of the separate species better, also the reduction of $NO_x^{-1390\ cm^{-1}}{}_{(ads)}$, and $NO_x^{-1305\ cm^{-1}}{}_{(ads)}$ was studied. $NO_2^-{}_{(aq)}$ was first adsorbed on passivated Pt/Al_2O_3, followed by flushing, (see top spectrum in Figure 3.[23,37] Clearly $NO_x^{-1390\ cm^{-1}}{}_{(ads)}$ and $NO_x^{-1305\ cm^{-1}}{}_{(ads)}$ were observed in agreement with previous results.[23] Subsequently, H_2/H_2O (4.1×10^{-6} mol/L H_2) was introduced into the cell to hydrogenate the preadsorbed $NO_x^-{}_{(ads)}$ species, and infrared peaks evolved as shown in Figures 3 and 4.

The bands of both $NO_x^{-1390\ cm^{-1}}{}_{(ads)}$ and $NO_x^{-1305\ cm^{-1}}{}_{(ads)}$ decreased quickly, and peaks developed at 2231 cm^{-1} (N_2O), 1620 cm^{-1} ($NO_{(ads)}^{1620\ cm^{-1}}$), and 1270 cm^{-1} ($HNO_2^-{}_{(ads)}$). Only very small amounts of "HNO"$_{(ads)}$ and NH_4^+ were detected, contrary to the experiment shown in Figure 2. $NO_{(ads)}^{1580\ cm^{-1}}$ was not observed at all in this experiment.

Further, the disappearance of $NO_x^{-1390\ cm^{-1}}{}_{(ads)}$ is much faster in this experiment (less than 4 min) as compared to the experiment in Figure 2 (over 30 min) in which also $NO_{(ads)}^{1580\ cm^{-1}}$ and "HNO"$_{(ads)}$ (1540 cm^{-1}) were present on the platinum surface at the start of the hydrogenation. Moreover, the platinum surface in Figure 3 was more oxidized than in Figure 2, because the adsorption in Figure 3 started on passivated Pt/Al_2O_3.

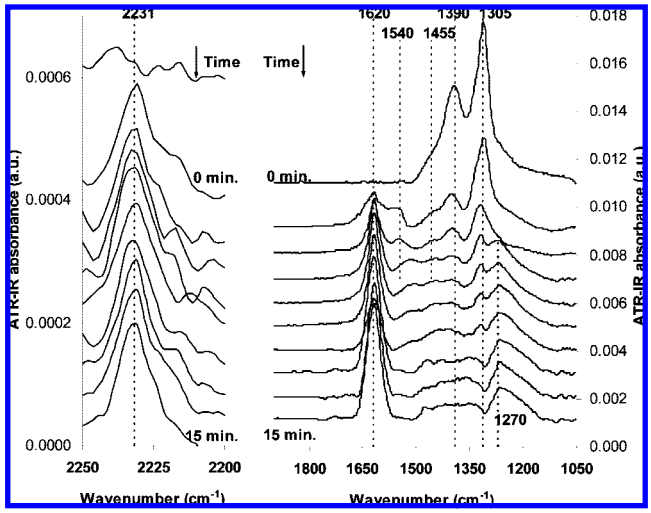

Figure 3. Water-corrected ATR-IR spectra while H_2/H_2O (4.1×10^{-6} mol/L H_2) was flown over Pt/Al_2O_3 with $NO_x^-{}_{(ads)}$, previously formed during adsorption of $NO_2^-{}_{(aq)}$ on Pt/Al_2O_3.[23] The integrated peak areas during flow of H_2/H_2O are shown in Figure 5.

Similar to the experiment presented in Figure 2, the intensity of $NO_{(ads)}^{1620\ cm^{-1}}$ decreased only very slowly during hydrogen flow for several hours. The peak at 1270 cm^{-1} decreased slightly (10%) during 15 min after which it stabilized, and N_2O was constantly being detected at a very low intensity. Since no other products were formed and N_2O is claimed to be an intermediate in the formation of N_2,[34,35] we suggest that $NO_{(ads)}^{1620\ cm^{-1}}$ is also a source for the formation of N_2, proceeding via N_2O.[34,35]

We have recently shown that N_2O is only weakly adsorbed (if adsorbed at all) and is flushed out of the cell during inert flow.[23,37] Continuing hydrogenation after 6 min, where only $NO_{(ads)}^{1620\ cm^{-1}}$ and $HNO_2^-{}_{(ads)}$ are present on the surface, the peak for N_2O was still detected, thus showing that N_2O is formed from either adsorbed $NO_{(ads)}^{1620\ cm^{-1}}$ and/or $HNO_2^-{}_{(ads)}$ in agreement with literature.[34,44−48] Moreover, the results in Figure 1 showed already that in the absence of $NO_{(ads)}^{1620\ cm^{-1}}$ N_2O is produced as well from $NO_{(ads)}^{1580\ cm^{-1}}$ or "HNO"$_{(ads)}$.

To study the effect of the presence of $NO_{(ads)}^{1620\ cm^{-1}}$ and $HNO_2^-{}_{(ads)}$ on the adsorption and subsequent hydrogenation of nitrite, the catalyst layer obtained at the end of experiment 3 was again exposed to $NO_2^-{}_{(aq)}$ and subsequently reduced. At the start of the experiment, the Pt surface contains $NO_{(ads)}^{1620\ cm^{-1}}$, $HNO_2^-{}_{(ads)}$, and $H_{(ads)}$.

Adsorption of $NO_2^-{}_{(aq)}$ results in the ATR-IR spectra shown in Figure 4A, with the integrated intensities shown in Figure 5. Instantly, $NO_{x(ads)}^{-1390\ cm^{-1}}$, "HNO"$_{(ads)}$, and NH_4^+ were observed; $HNO_2^-{}_{(ads)}$ almost doubled in intensity, and the peak of $NO_{(ads)}^{1620\ cm^{-1}}$ did not change at all. $NO_{x(ads)}^{-1305\ cm^{-1}}$ and $NO_{(ads)}^{1580\ cm^{-1}}$ were detected only after 3 min (i.e., at 23 min in Figure 5). (The peak for $HNO_2^-{}_{(ads)}$ (1270 cm^{-1}) is necessary for a good fit, whereas this is not the case for the experiment in Figure 1). While the intensity for $NO_{x(ads)}^{-1390\ cm^{-1}}$ is similar as after adsorption on a passivated Pt/Al_2O_3 surface[23] or $H-Pt/Al_2O_3$ (Figure 1), $NO_{x(ads)}^{-1305\ cm^{-1}}$ only reaches about 70% of its original intensity. Since at the start of this experiment $NO_{(ads)}^{1620\ cm^{-1}}$ and $HNO_2^-{}_{(ads)}$ are present on the catalyst surface, these species seem to inhibit the adsorption of $NO_{x(ads)}^{-1305\ cm^{-1}}$, which is reflected in both the delay in adsorption and the lower final intensity.

The formation of $NO_{x(ads)}^{-1390\ cm^{-1}}$, "HNO"$_{(ads)}$, NH_4^+, and $NO_{(ads)}^{1580\ cm^{-1}}$ resembles the experiment shown in Figure 1, in which nitrite was adsorbed onto a platinum surface covered with

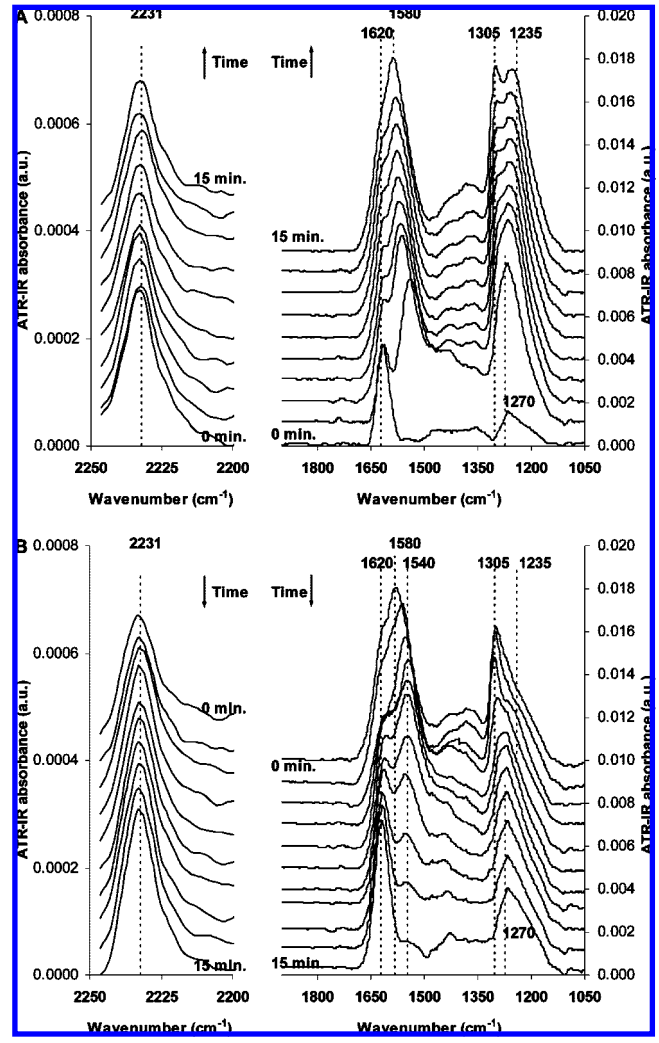

Figure 4. (A) Water-corrected ATR-IR spectra while a solution of $NO_2^-{}_{(aq)}$ (4.3×10^{-4} mol/L) at pH 7.0 was flown over Pt/Al_2O_3 with N_2O, $NO_{(ads)}^{1620\ cm^{-1}}$, and $HNO_2^-{}_{(ads)}$, previously formed during adsorption of $NO_2^-{}_{(aq)}$ on $H-Pt/Al_2O_3$ (Figure 1) and subsequent flow of H_2/H_2O (4.1×10^{-6} mol/L H_2) (Figure 3). The initial spectrum at time = 0 is identical to the last spectrum in Figure 3 at time = 15 min. (B) Water-corrected ATR-IR spectra during subsequent flow of H_2/H_2O (4.1×10^{-6} mol/L H_2) (after removal of $NO_2^-{}_{(aq)}$ by flushing).

hydrogen only. However, the relative amounts of the species formed differ; the ratio $NO_{(ads)}^{1580\ cm^{-1}}$/"HNO"$_{(ads)}$ decreased from 1.4 (Figure 1) to 0.9 (Figure 5).

After this second adsorption of $NO_2^-{}_{(aq)}$, H_2/H_2O was introduced into the cell. Figure 4B shows the time-resolved infrared spectra of this experiment; the integrated intensities can be found in Figure 5C.

Similar to the experiment shown in Figure 2, during hydrogenation, $NO_{x(ads)}^{-1305\ cm^{-1}}$ and $NO_{(ads)}^{1580\ cm^{-1}}$ decreased and "HNO"$_{(ads)}$ reached a maximum after about 6 min, after which it started to decrease as well. Simultaneously, the peak for NH_4^+ (1455 cm^{-1}) increased until a maximum at 10 min and then slowly decreased. Furthermore, the very slow decrease of $NO_{x(ads)}^{-1390\ cm^{-1}}$ is consistent with the experiment in Figure 2. At this point it is not clear to which products $NO_{x(ads)}^{-1390\ cm^{-1}}$ is converted.

The most prominent difference with Figure 2, is the fact that $NO_{(ads)}^{1620\ cm^{-1}}$ hardly increases during reduction, while $HNO_2^-{}_{(ads)}$ (1270 cm^{-1}) doubles in intensity. This changes the ratio of intensity of $NO_{(ads)}^{1620\ cm^{-1}}/HNO_2^-{}_{(ads)}$ (1270 cm^{-1}) from 2.5 (first adsorption/reduction cycle) to 0.6 (second

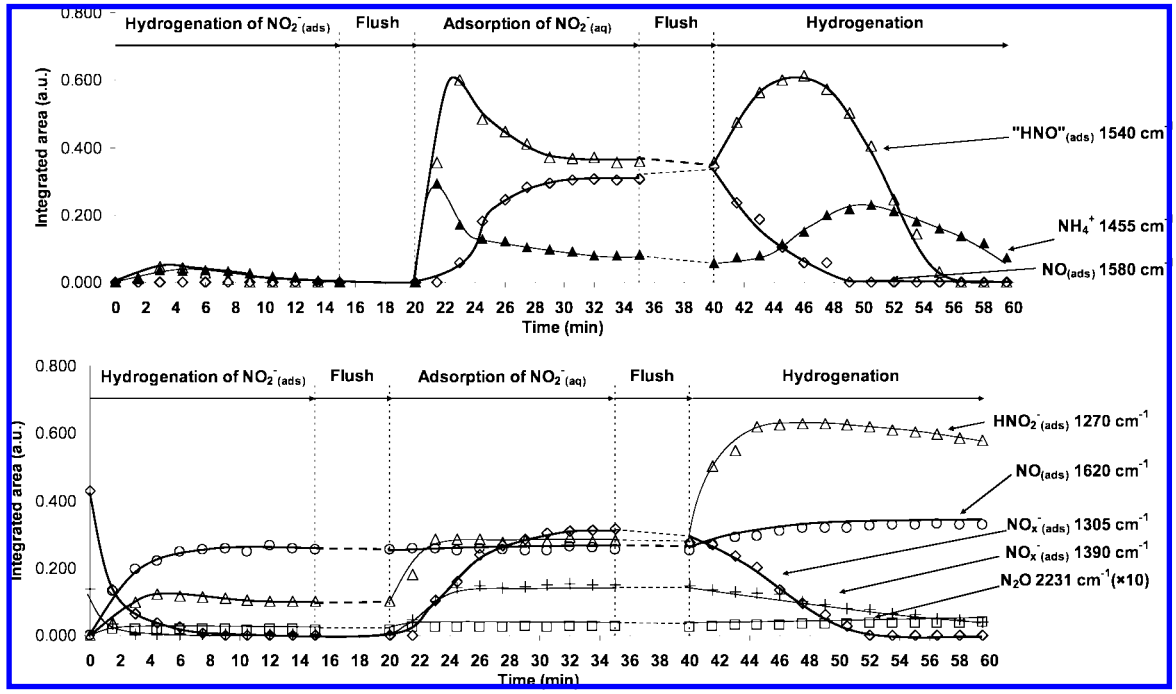

Figure 5. Integrated peak areas during hydrogenation of preadsorbed nitrite (Figure 4A, first 15 min), subsequent adsorption of $NO_2^-_{(aq)}$ (Figure 4A, 20−35 min) and the integrated peak area during the subsequent hydrogenation of the adsorbed species formed in Figure 4A (Figure 4B, 40−60 min).

adsorption/reduction cycle). Thus we propose that the presence of $NO^{1620\ cm^{-1}}_{(ads)}$ limits the conversion of $HNO_2^-_{(ads)}$. As already discussed above, $NO^{1620\ cm^{-1}}_{(ads)}$ is only very slowly hydrogenated, most likely to N_2O. This observation suggests reaction 3 given below, in which $NO^{1620\ cm^{-1}}_{(ads)}$ is accumulating because of the last rate determining step. At the start of the last experiment, shown in Figure 5, almost all Pt step sites are saturated by $NO^{1620\ cm^{-1}}_{(ads)}$. As a result, $HNO_2^-_{(ads)}$ cannot convert anymore into $NO^{1620\ cm^{-1}}_{(ads)}$ and thus will accumulate on the surface as observed. Since the time scale for the formation and removal of respectively $HNO_2^-_{(ads)}$ and $NO^{-1305\ cm^{-1}}_{x(ads)}$ are very similar, we suggest that $NO^{-1305\ cm^{-1}}_{x(ads)}$ is the main source for the production of $HNO_2^-_{(ads)}$

$$NO^{-}_{x(ads)}\ ^{1305cm^{-1}} \xrightarrow{H_2} HNO^{-}_{2(ads)} \xrightarrow{H_2}$$

$$NO_{(ads)}\ ^{1620cm^{-1}} \xrightarrow[\text{determining}]{\text{rate}} N_2O \quad (3)$$

As discussed at Figure 1, adsorbing nitrite on a hydrogen-covered Pt surface yields "HNO"$_{(ads)}$, $NO^{1580\ cm^{-1}}_{(ads)}$, and NH_4^+. On the other hand, Figures 2, 3, and 4 show that $NO^{-1305\ cm^{-1}}_{x(ads)}$ can be converted into $NO^{1620\ cm^{-1}}_{(ads)}$ when adding hydrogen to adsorbed $NO^{-1305\ cm^{-1}}_{x(ads)}$ on an initially hydrogen free platinum surface. Because of the much stronger absorption bands of $NO^{-1305\ cm^{-1}}_{x(ads)}$ and $NO_2^-_{(aq)}$ in Figure 2, the formation of "HNO"$_{(ads)}$ via $HNO_2^-_{(ads)}$ can not be excluded at this point.

Further, $NO^{1580\ cm^{-1}}_{(ads)}$ and $NO^{1620\ cm^{-1}}_{(ads)}$ are not significantly converted into each other in the presence of hydrogen, as can be seen in Figure 5, while large amounts of $NO^{1580\ cm^{-1}}_{(ads)}$ are converted, the signal of $NO^{1620\ cm^{-1}}_{(ads)}$ hardly changes in intensity. Moreover, Figure 1 showed that during nitrite adsorption only $NO^{1580\ cm^{-1}}_{(ads)}$ was formed, and $NO^{1620\ cm^{-1}}_{(ads)}$ could not be observed.

Continuous Hydrogenation of $NO_2^-_{(aq)}$ on H−Pt/Al_2O_3. Finally, continuous nitrite hydrogenation over H−Pt/Al_2O_3 was studied in situ. A solution of 4.3×10^{-4} mol/L $NO_2^-_{(aq)}$ and 4.1×10^{-4} mol/L H_2 was introduced into the cell with a freshly prepared prereduced H−Pt/Al_2O_3 layer. Figure 6 shows the ATR spectra with time and the integrated peak areas.

In three minutes, signals developed and stabilized for $NO_2^-_{(aq)}$, $NO^{-1390\ cm^{-1}}_{x(ads)}$, "HNO"$_{(ads)}$, NH_4^+, and N_2O. With a slight delay (after 6 min) also the peak for $NO^{-1305\ cm^{-1}}_{x(ads)}$ stabilized. As discussed above, the presence of $HNO_2^-_{(ads)}$ (1270 cm^{-1}) can not be excluded because of the presence of $NO_2^-_{(aq)}$ which has a very strong absorption band. However, the goodness of fit largely decreased when an additional band at 1270 cm^{-1} was added. The first 5 min of the experiment presented in Figure 6 represent a similar transient response as shown in Figure 1. After 6 min, when stable levels are observed, steady state hydrogenation is achieved.

On Pd/Al_2O_3 nitrite conversion was estimated to be around 4% under identical conditions (with a hydrogen conversion of 11% assuming selectivity to ammonia) based on nitrite conversion rates based on kinetic studies in a batch reactor.[49] Since platinum catalysts are reported to be comparable in activity to palladium catalysts for the hydrogenation of nitrite,[17] we conclude that the experiments in the present study are close to differential conditions as well.

Interestingly, during steady state hydrogenation neither $NO^{1620\ cm^{-1}}_{(ads)}$ nor $NO^{1580\ cm^{-1}}_{(ads)}$ is observed in contrast to the transient experiments presented above. The absence of $NO^{1620\ cm^{-1}}_{(ads)}$ can be explained by the fact that it also is not observed when adsorbing nitrite on a hydrogen-covered platinum surface (see Figure 1). Interestingly, the above experiments showed that $NO^{-1305\ cm^{-1}}_{x(ads)}$ is the likely reactant to produce $NO^{1620\ cm^{-1}}_{(ads)}$ (see eq 3). While in the transient experiments $NO^{1620\ cm^{-1}}_{(ads)}$ accumulates and is clearly visible, its absence during continuous hydrogenation is either due to fast conversion or an insignificant rate of formation. Since the transient experiments have clearly shown that

SCHEME 1: Suggested Reaction Scheme of the Catalytic Hydrogenation of Nitrite over Pt/Al_2O_3

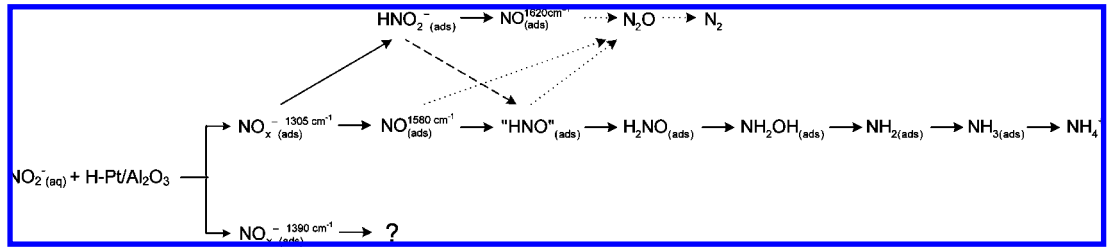

$NO_{(ads)}^{1620\ cm^{-1}}$ is only very slowly hydrogenated, we conclude that its formation does not take place under the applied conditions. The main difference between the transient and continuous hydrogenation experiments is the presence of $NO_2^-{}_{(aq)}$. Moreover, $NO_{(ads)}^{1620\ cm^{-1}}$ only develops in the transient experiments if $NO_{x(ads)}^{-1305\ cm^{-1}}$ disappears. During the continuous hydrogenation, however, the observed amount of $NO_{x(ads)}^{-1305\ cm^{-1}}$ is constant because of the presence of $NO_2^-{}_{(aq)}$. This observation suggests that $NO_{(ads)}^{1620\ cm^{-1}}$ is adsorbed on the same sites needed to convert $NO_{x(ads)}^{-1305\ cm^{-1}}$ with hydrogen. In any case, $NO_{(ads)}^{1620\ cm^{-1}}$ will not be an important intermediate for the conversion of nitrite over platinum, because of its very slow conversion as shown in Figures 2 and 4.

The absence of $NO_{(ads)}^{1580\ cm^{-1}}$ is probably due to the continuous presence of hydrogen as it was already shown that $NO_{(ads)}^{1580\ cm^{-1}}$ converts rapidly into "HNO"$_{(ads)}$ in the presence of hydrogen. Indeed "HNO"$_{(ads)}$ is clearly the dominant surface species (Figure 5). This also indicates that the hydrogenation of "HNO"$_{(ads)}$ to NH_4^+ is, at least partly, rate determining under the applied conditions. Finally, also during steady-state nitrite hydrogenation, N_2O is continuously formed.

Mechanism for Hydrogenation of Nitrite on Pt/Al_2O_3. Scheme 1 below summarizes the findings in this paper on the surface intermediates and possible reaction mechanism of the heterogeneous catalytic hydrogenation of nitrite in water over Pt/Al_2O_3 as obtained by in situ ATR-IR spectroscopy.

The scheme is based on the findings in the present study and discussion in literature.[27] The dotted lines represent possible reaction pathways for formation of "HNO"$_{(ads)}$, N_2O, and N_2, although at present there is no evidence for these pathways.

Adsorption of $NO_2^-{}_{(aq)}$ on H−Pt/Al_2O_3 yields adsorbed nitrite species and the hydrogenation products $NO_{(ads)}^{1580\ cm^{-1}}$, "HNO"$_{(ads)}$, NH_4^+, and N_2O as shown in Figure 1. The present study shows that $NO_{(ads)}^{1580\ cm^{-1}}$ on the platinum surface undergoes a stepwise hydrogenation process first to "HNO"$_{(ads)}$ and subsequently to NH_4^+ as the final hydrogenation product (Figure 2). Also electrochemical reduction of NO adlayers over platinum electrodes showed that $NO_{(ads)}^{1580\ cm^{-1}}$ is converted to "HNO"$_{(ads)}$ in the presence of hydrogen, while the reversed reaction occurs in the absence of hydrogen.[50]

It is clear that hydrogenation of nitrite via "HNO"$_{(ads)}$ to NH_4^+ must be a sequence of elementary reaction steps in which oxygen is removed and hydrogen is attached to the nitrogen atom. We have recently shown that formation of $NO_{(ads)}^{1580\ cm^{-1}}$ and "HNO"$_{(ads)}$ can arise from decomposition/reaction of NH_2OH on Pt/Al_2O_3.[23,37] Further, hydrogenation of nitrite to ammonia over Pd/Al_2O_3 also proceeds via NH_2OH.[15,23] While on Pt/Al_2O_3, "HNO"$_{(ads)}$ is detected in the reaction sequence to ammonia, on Pd/Al_2O_3, $NH_{2(ads)}$ was observed. These observations indicate that different steps in the formation of ammonia are rate limiting over platinum and palladium; hydrogenation of "HNO"$_{(ads)}$ to NH_4^+ is rate limiting for Pt/Al_2O_3, whereas the hydrogenation of $NH_{2(ads)}$ to NH_4^+ is rate limiting over Pd/Al_2O_3. Moreover, contrary to Pd/Al_2O_3, similar concentrations of hydrogen and nitrite show clear surface intermediates for Pt/Al_2O_3 during the continuous hydrogenation of nitrite (Figure 6). On Pd/Al_2O_3 the hydrogen concentration had to be lowered drastically to observe any surface intermediates. This also indicates that the rate determining step in the nitrite hydrogenation mechanisms occurs at different points in the sequence for platinum compared to palladium. On palladium the rate determining step is the activation of nitrite, unless the hydrogen pressure is extremely low. In that case the conversion of $NH_{2(ads)}$ into ammonia becomes rate limiting, and $NH_{2(ads)}$ is observed. On platinum the hydrogenation of HNO is rate limiting, even at higher hydrogen pressure.

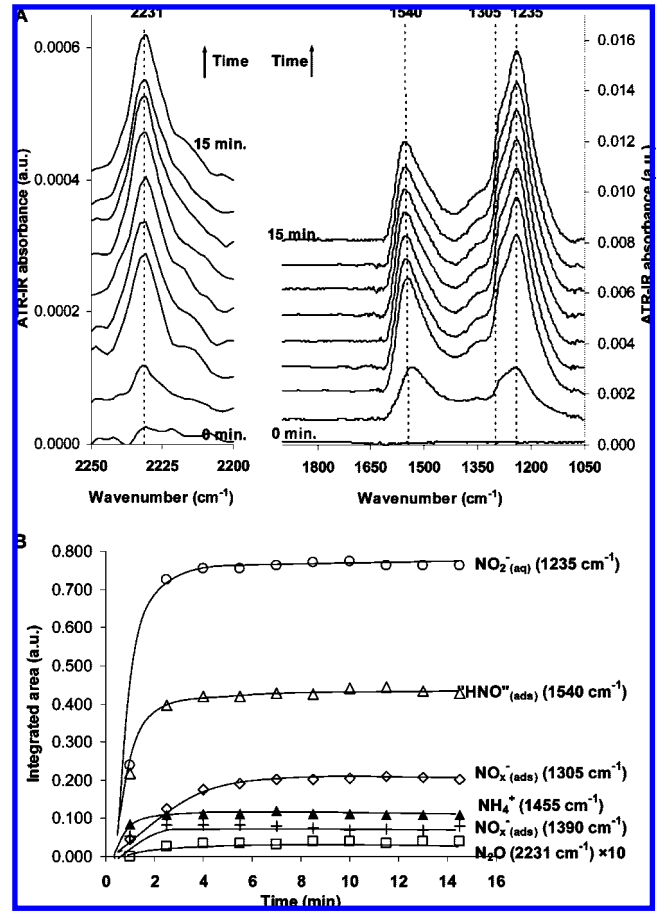

Figure 6. (A) Water-corrected ATR-IR spectra during hydrogenation of $NO_2^-{}_{(aq)}$ over H−Pt/Al_2O_3 (4.3×10^{-4} mol/L $NO_2^-{}_{(aq)}$ and 4.1×10^{-4} mol/L H_2) (the time between spectra was 1.5 min). (B) Integrated peak areas during hydrogenation.

From the present results, the mechanism for the formation of N_2O, which was detected during all hydrogenation experiments in this study, is not clear yet. N_2O can be formed either via dimerization of $NO_{(ads)}$ and/or "HNO"$_{(ads)}$ or via dissociation of NO on steps as proposed in literature.[16,29,35,39,45,51−58] Interest-

ingly, although they cannot be converted into each other, $NO_{(ads)}^{1580\ cm^{-1}}$ and $NO_{(ads)}^{1620\ cm^{-1}}$ both seem to lead to N_2O (Figure 1, Figure 2, Figure 3, and Figure 4). Dimerization of $NO_{(ads)}^{1580\ cm^{-1}}$ is easy to understand since the infrared signals show a dipole coupling effect, indicating that NO molecules are in each other vicinity. On the other hand, $NO_{(ads)}^{1620\ cm^{-1}}$ was assigned to NO adsorbed on steps sites, with no interaction between separate NO molecules. A dimerization into N_2O seems therefore unlikely. However, in the gas phase it was reported that NO dissociation normally is favored on stepped surfaces.[59−61] A similar reaction path for $NO_{(ads)}^{1620\ cm^{-1}}$ is suggested here; first NO dissociation and second formation of N_2O via reaction between N_{ads} and NO_{ads}.

The amounts of N_2O detected in this study are very low compared to the amounts of ammonia. This can be explained by the fact that N_2O is flushed out of the cell and that for $NO_{(ads)}^{1580\ cm^{-1}}$ the competitive reaction to ammonia is much faster than the dimerization into N_2O. $NO_{(ads)}^{1620\ cm^{-1}}$ reacts very slowly (Figure 2, 3, and 4). In addition, N_2O was demonstrated in literature to be an intermediate in the formation of nitrogen.[34,35] Therefore, nitrogen may form over Pt/Al_2O_3, but unfortunately nitrogen could not be detected here since it is not infrared active.

The reaction scheme of the heterogeneous hydrogenation of nitrite shown in Scheme 1 is similar to the schemes proposed for both heterogeneous hydrogenation of nitrite over supported noble metal catalysts [5,7,8,12] and electrochemical reduction of nitrite (and NO adlayers) on platinum electrodes.[27,32,62,63] For the first time, this study provides experimental evidence for some of the surface intermediates during the heterogeneous hydrogenation of nitrite over a supported platinum catalyst. Recently, we have shown that over Pd/Al_2O_3 the formation of nitrogen (via N_2O) and ammonia takes place via two independent pathways.[15,37] As described above, two different NO species are present on Pt/Al_2O_3 ($NO_{(ads)}^{1580\ cm^{-1}}$ and $NO_{(ads)}^{1620\ cm^{-1}}$). Both of these NO species are involved in the formation of N_2O, whereas $NO_{(ads)}^{1580\ cm^{-1}}$ hydrogenates to ammonia also, with "HNO"$_{(ads)}$ as an intermediate as was also proposed in literature.[5,7,8,12,27,32,62,63] On Pd/Al_2O_3, on the other hand, we recently showed that hydrogenation of NO does not result in ammonia, as ammonia is formed exclusively via a pathway including hydrogenation of $NH_{2(ads)}$ and excluding adsorbed NO.[15]

Furthermore on Pt/Al_2O_3 we suggest that $NO_{(ads)}$ can be formed from $HNO_2^-{}_{(ads)}$. Since $HNO_2^-{}_{(ads)}$ was not observed during hydrogenation of nitrite over Pd/Al_2O_3 in our previous study, the reaction pathway from $HNO_2^-{}_{(ads)}$ to $NO_{(ads)}$ was not discussed. A reaction pathway via $HNO_2^-{}_{(ads)}$ and $NO_{(ads)}$ on Pd/Al_2O_3 is very well possible. Apparently, on palladium the hydrogenation of $HNO_2^-{}_{(ads)}$ to $NO_{(ads)}$ is faster than the consecutive hydrogenation of $NO_{(ads)}$, in contrast to hydrogenation of nitrite over Pt/Al_2O_3, where the hydrogenation of $HNO_2^-{}_{(ads)}$ occurs very slowly (Figure 2 and Figure 5).

The main goal of this study was to evaluate the nitrite hydrogenation mechanism over Pt/Al_2O_3 as proposed in literature[6,12−14] by identifying adsorbed intermediates. Clearly, on Pt/Al_2O_3 the mechanism is complex and involves a number of pathways, some of them connected via adsorbed species and leading to ammonia and N_2O. Further, the heterogeneous catalytic mechanism seems to resemble the electrochemical nitrite/nitrate reduction over platinum electrodes literature.[5,7,8,12,27,32,62,63] Moreover, the results show that although the reaction pathways of nitrite hydrogenation on platinum and palladium are rather similar, the rate determining steps are clearly different.

Conclusion

The surface intermediates during the heterogeneous hydrogenation of nitrite over Pt/Al_2O_3 were investigated in water by ATR-IR spectroscopy. In addition to adsorbed nitrite, $NO_{(ads)}$, "HNO"$_{(ads)}$, $HNO_2^-{}_{(ads)}$, and NH_4^+ are formed on the platinum surface. Hydrogenation of nitrite yields ammonia via a stepwise hydrogenation process via $NO_{(ads)}$ and "HNO"$_{(ads)}$ as intermediates, with hydrogenation of "HNO"$_{(ads)}$ as the rate-determining step. Very slow conversion of $NO_{(ads)}$ to N_2O was also detected. A nonreactive NO species adsorbed platinum steps was detected in transient experiments but not during steady state operation. The results, furthermore, indicate that the reaction pathway of nitrite hydrogenation on platinum and palladium is rather similar, but the rate determining steps are definitely different.

References and Notes

(1) Bruning-Fann, C. S.; Kaneene, J. B. *Vet. Hum. Toxicol.* **1993**, *35*, 521.
(2) World Health Organization. *Water and health in Europe*, WHO, Regional Office for Europe, Copenhagen (2002).
(3) World Health Organization. *Nitrate and nitrite in Drinking-water*, WHO, Regional Office for Europe, Copenhagen (2003).
(4) Hörold, S.; Vorlop, K. D.; Tacke, T.; Sell, M. *Catal. Today* **1993**, *17*, 21.
(5) Wärnå, J.; Turunen, I.; Salmi, T.; Maunula, T. *Chem. Eng. Sci.* **1994**, *49*, 5763.
(6) Daum, J.; Vorlop, K. D. *Chem. Eng. Technol.* **1999**, *22*, 199.
(7) Hörold, S.; Tacke, T.; Vorlop, K. D. *Environ. Technol.* **1993**, *14*, 931.
(8) Vorlop K. D.; Prusse,U. 1999.
(9) Hahnlein, M.; Prusse, U.; Daum, J.; Morawsky, V.; Koger, M.; Schroder, M.; Schnabel, M.; Vorlop, K. D. 1998.
(10) Prüsse, U.; Daum, J.; Bock, C.; Vorlop, K. D. *Stud. Surf. Sci. Catal.* **2000**, *130*, 2237.
(11) Pintar, A.; Batista, J.; Levec, J. *Water. Sci. Technol.* **1998**, *37*, 177.
(12) Pintar, A.; Batista, J.; Levec, J.; Kijiuchi, T. *Appl. Catal., B* **1996**, *11*, 81.
(13) Prüsse, U.; Hahnlein, M.; Daum, J.; Vorlop, K. D. *Catal. Today* **2000**, *55*, 79.
(14) Daub, K.; Emig, G.; Chollier, M. J.; Callant, M.; Dittmeyer, R. *Chem. Eng. Sci.* **1999**, *54*, 1577.
(15) Ebbesen, S. D.; Mojet, B. L.; Lefferts, L. *J. Catal.* **2008**, *256*, 15.
(16) de Vooys, A. C. A.; Koper, M. T. M.; van Santen, R. A.; van Veen, J. A. R. *J. Catal.* **2001**, *202*, 387.
(17) D'Arino, M.; Pinna, F.; Strukul, G. *Appl. Catal., B* **2004**, *53*, 161.
(18) Harrick, N. J. *Internal Reflection Spectroscopy*; Interscience Publishing: New York, 1967.
(19) Baird, A. S. *J. Phys. Chem. C* **2007**, *111*, 14207.
(20) Ebbesen, S. D.; Mojet, B. L.; Lefferts, L. *J. Catal.* **2007**, *246*, 66.
(21) He, R.; Davda, R. R.; Dumesic, J. A. *J. Phys. Chem. B.* **2005**, *109*, 2810.
(22) Ferri, D.; Bürgi, T.; Baiker, A. *J. Catal.* **2002**, *210*, 160.
(23) Ebbesen, S. D.; Mojet, B. L.; Lefferts, L. *Langmuir* **2008**, *24*, 869.
(24) Bürgi, T.; Baiker, A. *J. Phys. Chem. B.* **2002**, *106*, 10649.
(25) Ortiz-Hernandez, I.; Williams, C. T. *Langmuir* **2003**, *19*, 2956.
(26) Ferri, D.; Bürgi, T.; Baiker, A. *J. Phys. Chem. B* **2001**, *105*, 3187.
(27) Rosca, V.; Koper, M. T. M. *Surf. Sci.* **2005**, *584*, 258.
(28) da Cunha, M.C.P.M.; Weber, M.; Nart, F. C. *J. Electroanal. Chem.* **1996**, *414*, 163.
(29) da Cunha, M.C.P.M.; De Souza, J. P. I.; Nart, F. C. *Langmuir* **2000**, *16*, 771.
(30) Gomez, R.; Rodes, A.; Orts, J. M.; Feliu, J. M.; Perez, J. M. *Surf. Sci.* **1995**, *342*, L1104.
(31) Rosca, V.; Koper, M. T.M. *J. Phys. Chem. B.* **2005**, *109*, 16750.
(32) Rosca, V.; Beltramo, G. L.; Koper, M. T. M. *Langmuir* **2005**, *21*, 1448.
(33) Weaver, M. J.; Zou, S. Z.; Tang, C. *J. Chem. Phys.* **1999**, *111*, 368.
(34) Bae, I. T.; Barbour, R. L.; Scherson, D. A. *Anal. Chem.* **1997**, *69*, 249.
(35) de Vooys, A. C. A.; Koper, M. T. M.; van Santen, R. A.; van Veen, J. A. R. *Electrochim. Acta* **2001**, *46*, 923.
(36) Ebbesen, S. D.; Mojet, B. L.; Lefferts, L. *Langmuir* **2006**, *22*, 1079.
(37) Ebbesen, S. D. *Spectroscopy under the Surface - In-Situ ATR-IR Studies of Heterogeneous Catalysis in Water, Doctoral Thesis*; Gildeprint, B. V.; Enschede: 2007.
(38) Begun, G. M.; Fletcher, W. H. *J. Chem. Phys.* **1958**, *28*, 414.

(39) Rosca, V.; Beltramo, G. L.; Koper, M. T. M. *J. Electroanal. Chem.* **2004**, *566*, 53.
(40) Rodes, A.; Gomez, R.; Orts, J. M.; Feliu, J. M.; Perez, J. M.; Aldaz, A. *Langmuir* **1995**, *11*, 3549.
(41) Matatov-Meytal, Y.; Barelko, V.; Yuranov, I.; Sheintuch, M. *Appl. Catal., B* **2000**, *27*, 127.
(42) Matatov-Meytal, Y.; Shindler, Y.; Sheintuch, M. *Appl. Catal., B* **2003**, *45*, 127.
(43) Dima, G. E.; Beltramo, G. L.; Koper, M. T. M. *Electrochim. Acta* **2005**, *50*, 4318.
(44) Ye, S.; Kita, H. *J. Electroanal. Chem.* **1993**, *346*, 489.
(45) Gootzen, J. F. E.; van Hardeveld, R. M.; Visscher, W.; van Santen, R. A.; van Veen, J. A. R. *Recl. Trav. Chim. Pays-Bas* **1996**, *115*, 480.
(46) Nishimura, K.; Machida, K.; Enyo, M. *Electrochim. Acta* **1991**, *36*, 877.
(47) Balbaud, F.; Sanchez, G.; Santarini, G.; Picard, G. *Eur. J. Inorg. Chem.* **2000**, 665.
(48) Rodes, A.; Gomez, R.; Orts, J. M.; Feliu, J. M.; Aldaz, A. *J. Electroanal. Chem.* **1993**, *359*, 315.
(49) Pintar, A.; Bercic, G. *AIChE J.* **1998**, *44*, 2280.
(50) Beltramo, G. L.; Koper, M. T. M. *Langmuir* **2003**, *19*, 8907.
(51) Janssen, L. J. J.; Pieterse, M. M. J.; Barendrecht, E. *Electrochim. Acta* **1977**, *22*, 27.
(52) Paseka, I.; Vonkova, J. *Electrochim. Acta* **1980**, *25*, 1251.
(53) Paseka, I.; Hodinar, A. *Electrochim. Acta* **1982**, *27*, 1461.
(54) Colucci, J. A.; Foral, M. J.; Langer, S. H. *Electrochim. Acta* **1985**, *30*, 521.
(55) de Vooys, A. C. A.; Beltramo, G. L.; van Riet, B.; van Veen, J. A. R.; Koper, M. T. M. *Electrochim. Acta* **2004**, *49*, 1307.
(56) MacNeil, J. H.; Berseth, P. A.; Westwood, G.; Trogler, W. C. *Environ, Sci. Technol.* **1998**, *32*, 876.
(57) Kuwabata, S.; Uezumi, S.; Tanaka, K.; Tanaka, T. *Inorg. Chem.* **1986**, *25*, 3018.
(58) De, D. D.; Englehardt, J. D.; Kalu, E. E. *J. Electrochem. Soc.* **2000**, *147*, 4573.
(59) Park, Y. O.; Banholzer, W. F.; Masel, R. I. *Appl. Surf. Sci.* **1984**, *19*, 145.
(60) Gohndrone, J. M.; Park, Y. O.; Masel, R. I. *J. Catal.* **1985**, *95*, 244.
(61) Gorte, R. J.; Schmidt, L. D.; Gland, J. L. *Surf. Sci.* **1981**, *109*, 367.
(62) Rodes, A.; Gomez, R.; Perez, J. M.; Feliu, J. M.; Aldaz, A. *Electrochim. Acta* **1996**, *41*, 729.
(63) Casero, E.; Alonso, C.; Martin-Gago, J. A.; Borgatti, F.; Felici, R.; Renner, F.; Lee, T. L.; Zegenhagen, J. *Surf. Sci.* **2002**, *507−510*, 688.

JP8081886